Shallow Sink in an Antenna Pigment System of Photosystem I of a Marine Centric Diatom, Chaetoceros gracilis, Revealed by Ultrafast Fluorescence Spectroscopy at 17 K

ARTICLE *in* THE JOURNAL OF PHYSICAL CHEMISTRY B · JULY 2010

Impact Factor: 3.3 · DOI: 10.1021/jp102205v · Source: PubMed

7 AUTHORS, INCLUDING:

Hiroyuki Koike
Chuo University
39 PUBLICATIONS **1,016** CITATIONS
SEE PROFILE

Shigeru Itoh
Nagoya University
222 PUBLICATIONS **4,114** CITATIONS
SEE PROFILE

Shallow Sink in an Antenna Pigment System of Photosystem I of a Marine Centric Diatom, *Chaetoceros gracilis*, Revealed by Ultrafast Fluorescence Spectroscopy at 17 K

Atsushi Yamagishi,[†] Yohei Ikeda,[‡,§] Masayuki Komura,[†] Hiroyuki Koike,[‡,∥] Kazuhiko Satoh,[‡] Shigeru Itoh,[†] and Yutaka Shibata*[,†]

Division of Material Science (Physics), Graduate School of Science, Nagoya University, Nagoya 464-8602, and Graduate School of Life Science, University of Hyogo, 3-2-1 Kouto, Kamigori-cho, Ako-gun, Hyogo 678-1297, Japan

Received: March 11, 2010; Revised Manuscript Received: May 31, 2010

The ultrafast fluorescence dynamics of photosystem I (PS I) purified from a marine centric diatom, *Chaetoceros gracilis*, at 17 K was studied using fluorescence up-conversion and streak-camera setups. The experiments were done for two kinds of sample preparations containing different amounts of the peripheral antenna proteins, the fucoxanthin−chlorophyll (Chl) binding proteins associated with PS I (FCPI). Upon excitation at 430 nm, which selectively excites Chl *a* mainly contained in the core complex, the fluorescence dynamics of both samples was roughly expressed by four decay-associated spectra (DASs) with time constants of ca. 5, ca. 22, ca. 100, and ca. 400 ps. These DAS components have corresponding counterparts in the results of a previous study of *Thermosynechococcus elongatus* PS I (Shibata et al. *J. Phys. Chem. B* **2010**, *114*, 2954) except for that with a time constant of ca. 22 ps. The similar distribution of the time constants suggests a shared light-harvesting pathway by PS I of these two organisms. The DAS with a ca. 400 ps time constant has its peak wavelength at around 710 nm, suggesting the presence of antenna pigment states with slightly lower excitation energy than that of P700. This antenna state acts as a shallow sink in the core complex of the diatom PS I and causes a specific temperature dependence of its fluorescence spectrum below 77 K. Excitation energy funneling into the shallow-sink state seems to take place within 0.2 ps, suggesting an extremely efficient energy transfer. Upon the selective excitation of Chl *c* in FCPI by a 460 nm laser, three DAS components suggesting excitation energy transfers were obtained. The 0.2 ps DAS shows the energy transfer from Chl *c* to Chl *a* within FCPI, while the 0.7 and 40 ps DASs suggest the energy transfer from FCPI to the core complex. The excitation energy seems to be effectively transferred from FCPI to the core complex in diatom PS I because the selective excitation of Chl *c* in FCPI does not induce a severe retardation of the overall light-harvesting kinetics.

Introduction

Diatoms are major hydrophytic photosynthesis microorganisms living abundantly in a wide variety of environments. They account for about 20% of the global carbon fixation[1,2] and have a considerable influence on the regulation of the global climate.[3] Diatoms have gained specific accessory pigments, such as chlorophyll (Chl) *c*, fucoxanthin, diatoxanthin, or diadinoxanthin, through their evolutional process. These accessory pigments are attached to unique light-harvesting proteins, the fucoxanthin−Chl binding proteins (FCPs),[4] which are members of the light-harvesting Chl protein (LHC) superfamily.[5] Recently, FCPs were confirmed to be associated with photosystem (PS) I as well as PS II.[6]

Diatoms are known to have unique acclimation mechanisms to changes in the environmental light conditions. In many oxygen-evolving photosynthetic organisms, including cyanobacteria, red algae, green algae, and higher plants, the stoichiometric ratio of PS II to PS I decreases when the light intensity decreases. In diatoms, on the contrary, the ratio increases when the light intensity decreases.[7,8] The unique acclimation strategy of diatoms might be related to their unique light-harvesting system. Specific carotenoids are suggested to be important for their unique protection mechanism of photosystems under high irradiance.[9−12] Diatoms are also known to have a characteristic arrangement of the thylakoid membrane, which shows no appreciable organization into the stacked granal region and the stroma-exposed region.[13−15]

In spite of the growing scientific interest, there have only been a few reports about the biophysical and biochemical characterization of the diatom photosynthetic apparatus. This is due to the difficulty in isolating intact photosynthetic pigment−protein complexes.[16] The difficulty is caused by the fact that cells of diatoms are covered with hard silicate shells. Recently, Ikeda et al. succeeded in isolating highly photoactive thylakoid membranes from a marine centric diatom, *Chaetoceros gracilis*.[6,17] They revealed that the cells of *C. gracilis* could be effectively disrupted by a freeze−thaw treatment. On the basis of this procedure, they succeeded in isolating the PS I reaction center complex. The isolated *C. gracilis* PS I complex was found to contain tightly bound FCP. In the present paper, we designate FCP associated with PS I as FCPI.

* To whom correspondence should be addressed. Phone/fax: 81-52-789-2883. E-mail: yshibata@bio.phys.nagoya-u.ac.jp.
[†] Nagoya University.
[‡] University of Hyogo.
[§] Present address: RIKEN Harima Institute Spring-8 Center, 1-1-1 Kouto, Sayo-cho, Sayo-gun, Hyogo 679-5148, Japan.
[∥] Present address: Department of Bioscience, Faculty of Science and Engineering, University of Chuo, 1-13-27 Kasuga, Bunkyo-ku, Tokyo 112-8551, Japan.

10.1021/jp102205v
Published on Web 06/17/2010

Interestingly, PS I of *C. gracilis* lacks the red-most-absorbing states, which we call hereafter "red Chl's". Red Chl's, which are typical for PS I of various organisms, have a much lower excited-state energy than the putative primary electron donor, P700. It has been long debated whether the light-harvesting kinetics of PS I is trap-limited[18,19] or transfer-to-trap-limited.[20,21] The influence of red Chl's on the overall light-harvesting dynamics in PS I has been a crucial issue. At cryogenic temperature, the fluorescence emission of PS I is dominated by that of red Chl's because the excitation energy captured by an antenna pigment is efficiently funneled into red Chl's. Although red Chl's have a considerable influence on the overall light-harvesting kinetics of PS I, their biological role has not been clarified. PS I of many cyanobacteria contains red Chl's, but an exception to this, i.e., PS I of *Gloeobacter violaceus*, has been reported.[22] PS I of *C. gracilis* is another example lacking red Chl. PS I of green algae has been known to show a wide variety with respect to the presence of red Chl's.[23] Thus, the presence of red Chl's is highly species-dependent.

Recently, we studied the excitation energy transfer (EET) kinetics in a trimeric PS I complex of a thermophilic cyanobacterium, *Thermosynechococcus elongatus*, at cryogenic temperature using ultrafast fluorescence spectroscopy.[24] *T. elongatus* PS I contains 7−11 molecules of Chl's that are assigned to red Chl's. Our study was particularly effective for the elucidation of EET through red Chl's because of the suppression of the uphill energy transfer at cryogenic temperature. In that study, we showed that the investigation of the fluorescence dynamics of PS I containing the oxidized P700 ($P700^+$) was very useful in revealing the energy-transfer pathway through the red Chl's. We identified three kinetically distinct red Chl's which transfer the excitation energy to $P700^+$ with time constants of 6.1, 140, and 360 ps. The energy flow through the red Chl with a time constant of 6.1 ps was found to be the major light-harvesting path in PS I containing oxidized P700.

The way in which the absence of red Chl's affects the EET kinetics of PS I is quite interesting. In the present study, we investigate the EET dynamics of PS I of a diatom, *C. gracilis*, using cryogenic ultrafast fluorescence spectroscopy. In addition to the *C. gracilis* PS I preparation by a method reported previously,[17] we here use a sample with a considerably reduced content of FCPI attached to the core complex. The samples were obtained by treatment of the crude *C. gracilis* PS I sample with a high-concentration detergent.[6] The EET process from FCPI to the core complex is deduced from the comparison of the data of these two samples. We compared the results of the two excitation wavelengths, namely, 430 and 460 nm. The light at the former wavelength selectively excites the Chl *a* mainly contained in the core complex, while the light at the latter exclusively excites Chl *c* in the peripheral antenna FCPIs. The EET process within the core complex is compared with that of the cyanobacterial PS I studied in previous work.[24] We will discuss how the absence of red Chl's affects the light-harvesting dynamics in the *C. gracilis* PS I.

Materials and Methods

The PS I sample was purified from *C. gracilis* as described elsewhere.[6,17] Briefly, thylakoid membranes were precipitated by centrifugation from the frozen−thawed cell suspension in the presence of DNase and protease inhibitor. The thylakoid membranes were solubilized with 0.85−0.95% (w/v) *n*-dodecyl *β*-D-maltopyranoside (DDM) for 10 min on ice. The PS I samples were purified by subsequent stepwise sucrose density-gradient centrifugation and anion-exchange chromatography. The PS I preparation obtained by the above procedure contains tightly bound FCPI and, hereafter, is called "FCPI-PS I". The FCPI-PS I preparation is basically the same as that used in the fluorescence dynamics study described in a previous paper.[17] In the present study, however, we purified the sample using anion-exchange chromatography instead of the gel filtration method used in the previous study.[17] This slight modification resulted in a significantly reduced content of fluorescence component from the uncoupled Chl's. To reduce the content of the bound FCPI, the FCPI-PS I sample was further solubilized by DDM with a final concentration of 15% (w/v).[6] After dilution of DDM to 0.5% (w/v), PS I with a reduced FCPI content was obtained by filtration with a cutoff molecular weight of 30 000 and 100 000. Hereafter, the PS I preparation obtained by the above-described additional purification procedure is called "PS I-core". The polypeptide compositions of both preparations were analyzed by electrophresis.[6] The analyses showed that the solubilization by a high concentration of DDM resulted in reduction of the FCPI content and loss of the PsaO subunit, while the other PS I subunits were shown to be maintained in the PS I-core preparation. The intactness of the P700 activities of both samples were confirmed by flash photolysis measurements.[6]

The instrumental setup for the observation of the fluorescence dynamics at cryogenic temperatures was described previously.[24−26] Our system is composed of a combination of fluorescence up-conversion and streak-camera (C4334, Hamamatsu Photonics Inc., Hamamatsu, Japan) setups. The sample excitation was done by the frequency-doubled light from a tunable Ti:sapphire laser (MaiTai, Spectra-Physics, Mountain View, CA) with a repetition rate of 80 MHz. Fluorescence dynamics over a very wide temporal range from 100 fs to 10 ns can be obtained by combining the data obtained by the two setups. The signal intensity was slightly decreased after a 15 min accumulation of data, probably due to spectral hole-burning at the exciting wavelengths. Typical decreases in the signal intensity are shown in the right panel of Figure S1 in the Supporting Information. After 1 h of data accumulation, the signal intensity decreased by about 30%. However, the shapes of the normalized time profiles, shown in the left panel of Figure S1, were hardly affected by the signal decrease. We moved the sample position after each 1 h data accumulation to measure the fresh sample position. The results are analyzed by the global fitting procedure, in which the observed fluorescence−time profiles at respective wavelengths are fitted to the sum of exponential functions.[24,26] In the fitting analysis, we constrained the time constants to have the same values among time profiles at different monitoring wavelengths. After this global fitting procedure, we obtained the decay-associated spectra (DASs), which are the plots of the pre-exponential factors vs the monitoring wavelengths.

The PS I samples were dissolved in a buffer (50 mM MES−NaOH pH 6.0) containing 10 mM $MgCl_2$, 5 mM $CaCl_2$, and 0.05% DDM. An aliquot of sodium ascorbate and methoxy-PMS was added to the sample solution to maintain P700 in its reduced state. Finally, the sample solution was mixed with 66% glycerol (v/v) and contained in a closed-cycle refrigerator system (model V202C5L, Daikin Industries, Ltd., Osaka, Japan). The optical path length was about 1 mm, and the optical density of the sample was set to less than 0.2 (per mm) to avoid the reabsorption effect.

Results

In Figure 1, we compared the absorption spectra between FCPI-PS I and PS I-core preparations. Fucoxanthins in FCPI

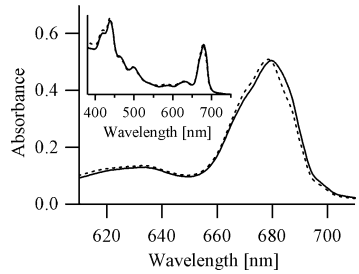

Figure 1. Absorption spectra in the Q_y region of FCPI-PS I (solid lines) and PS I-core (dashed lines) preparations at 5 K. Those over a wider spectral range are shown in the inset.

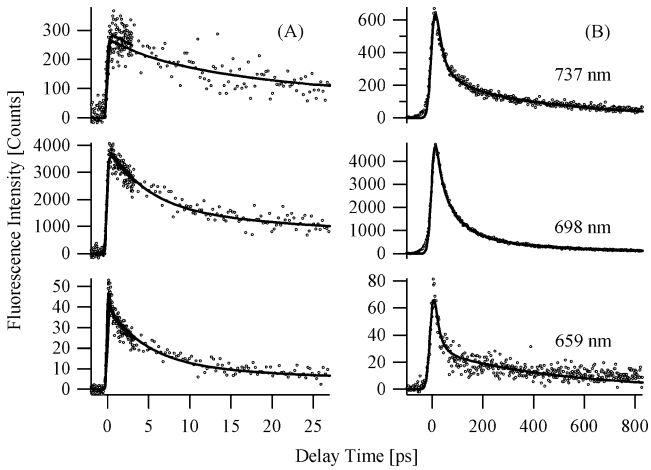

Figure 2. Fluorescence decay profiles (open circles) of FCPI-PS I at 17 K observed by the up-conversion (A) and the streak-camera (B) setups at 659 nm (traces at the bottom), 698 nm (traces in the middle), and 737 nm (traces at the top). The excitation wavelength was 430 nm. Solid lines are the fitting curves to the sum of the exponential functions.

are responsible for the spectral peak at around 500 nm. The main band in the Soret region at around 430 nm is due to Chl *a*, while the sub-band at around 460 nm is mainly contributed by the Soret band of Chl *c* in FCPI. The latter band might also contain the contribution from fucoxanthin. The different FCPI contents between the two preparations were mainly reflected in the slight difference in the Q_y absorption band of Chl *a* at around 680 nm. The spectral differences in the Chl *c* and fucoxanthin spectral regions were very slight, since the contents of both pigments were only minor in FCPI. The excitations at 430 and 460 nm result in the selective excitations of Chl *a* and Chl *c*, respectively.

Figure 2 shows the fluorescence decay dynamics of FCPI-PS I excited at 430 nm at 17 K. Panels A and B show the data obtained by the up-conversion setup and by the streak-camera setup, respectively. In the present study, the excitation power was set at 5 mW for the up-conversion measurement and at 2 mW for the streak-camera measurement. The diameter of the focal spot of the excitation laser was roughly estimated to be 40 μm. As shown in a previous paper,[24] this excitation power results in the oxidation of practically all P700 in the excited volume of the sample. The above estimation was based on the kinetic parameters of the charge-recombination reaction of PS I at cryogenic temperature.[27] Thus, we observed the EET dynamics with the oxidized P700 ($P700^+$) under the present experimental condition. $P700^+$ is known to be an effective quencher of the fluorescence of PS I[28] because it has a broad absorption band beyond 800 nm[29,30] and functions as an energy acceptor from antenna Chl's through a Förster-type EET

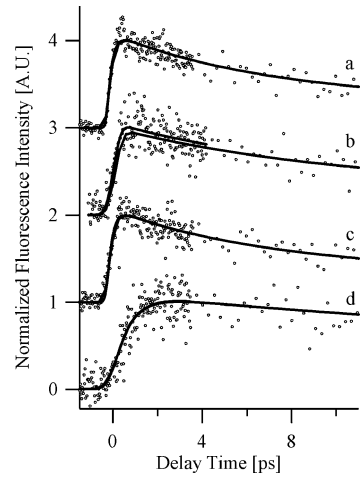

Figure 3. Fluorescence decay profiles (open circles) at 688 nm of PS I-core excited at 430 nm (trace a) and 460 nm (trace b) and those of FCPI-PS I excited at 430 nm (trace c) and 460 nm (trace d) observed by the up-conversion setup. The peak intensities were normalized to unity. Solid lines are the fitting curves to the sum of the exponential functions.

mechanism. On the other hand, P700 in the neutral form has an absorption band at around 700 nm and cannot be an energy acceptor from the red Chl's. At cryogenic temperature, therefore, the lifetime of the red Chl fluorescence becomes several nanoseconds when P700 is in the neutral form, while it is much faster when P700 is in the oxidized form.

The solid lines in Figure 2 are the fitting to the sum of the exponential functions. The fitting curves accurately reproduced the observed decays over a very wide temporal range. The data by the up-conversion system indicated that the fluorescence decay was almost completed within 10 ps at all monitoring wavelengths under this excitation condition. The rise time of the fluorescence was comparable to the instrumental response of 200 fs, suggesting a rapid exciton equilibration over the whole pigment system. This tendency is similar to that observed for the fluorescence dynamics of PS I of *T. elongatus* at 15 K.[24] We confirmed that the fluorescence−time profile was not affected by the change in the excitation power from 5 mW (63 pJ/pulse) to 2 mW (25 pJ/pulse). This clearly showed that the observed fast fluorescence decay was not contributed from the singlet−singlet annihilation. When the FCPI-PS I sample was excited at a 460 nm laser pulse, which selectively excites Chl *c* in the peripheral antenna FCPI, a slower fluorescence rise phase became observable. In Figure 3, we compare the fluorescence dynamics at 688 nm between different samples and different excitation wavelengths. An appreciable rise phase is seen only in trace d at the bottom of Figure 3, which is the fluorescence decay of FCPI-PS I excited at 460 nm. The rise time was estimated to be 0.7 ps.

Figure 4 shows the DASs of PS I-core excited at 430 nm (A) and 460 nm (B) and those of FCPI-PS I excited at 430 nm (C) and 460 nm (D) at 17 K. The DAS with a time constant around 0.2 ps, shown by the open circles, was always necessary to fit the observed time profiles. Since the fastest time constant was comparable to the instrumental response time, we did not set the value to be free to vary but fixed it to 0.2 ps. Slow DAS components with time constants of around 2 ns were necessary to fit the data of the PS I-core sample, while such components were absent for the FCPI-PS I sample. The slow components with ca. 2 ns time constants might originate from the antenna Chl that was uncoupled from the primary donor pigment. Treatment with detergent to reject the peripheral antenna might

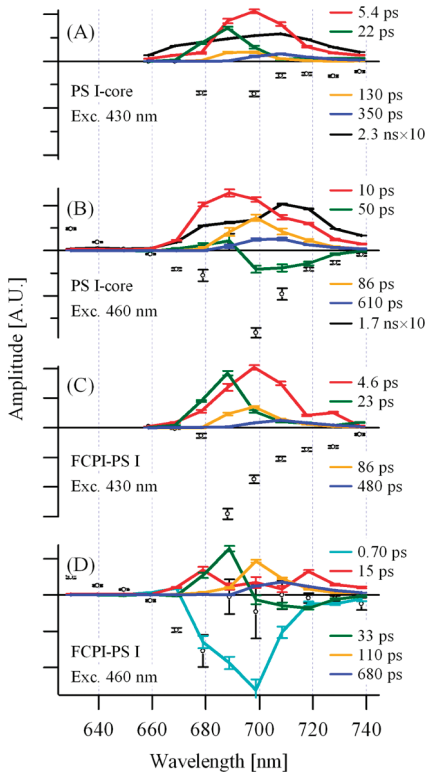

Figure 4. DASs of PS I-core excited at 430 nm (A) and 460 nm (B) and those of FCPI-PS I excited at 430 nm (C) and 460 nm (D). The black open circles show the DAS of the fastest component with a fixed time constant of 0.2 ps. The DASs with time constants of 2.3 ns in (A) and of 1.7 ns in (B) are magnified by a factor of 10 for comparison.

have caused the formation of such uncoupled Chl molecules in the PS I-core sample. The resultant parameters are summarized in Table 1.

Excitation at 430 nm resulted in essentially the same DAS profiles for PS I-core and FCPI-PS I samples except for the slowest 2.3 ns component. Thus, the fluorescence−time profile with Chl *a*-selective excitation was shown to be insensitive to the content of the peripheral antenna. This is consistent with the assumption that the 430 nm laser exclusively excites the pigments in the core complex but does not effectively excite those in the peripheral antenna. There was no DAS component showing the EET pattern in the case of the Chl *a*-selective excitation at 430 nm, suggesting rapid excitation energy equilibration. In the case of 460 nm Chl *c*-selective excitation, on the other hand, we saw several DAS components with an EET pattern: 630 nm (+) to 680 nm (−) with a time constant of 0.2 ps and 690 nm (+) to 710 nm (−) with time constants of around 20−50 ps. The DAS component with a time constant of 0.70 ps has a negative peak at around 700 nm and suggests the EET nature.

Figure 5 shows the temperature dependence of the fluorescence dynamics of PS I-core (left panels) and FCPI-PS I (right panels) observed by the streak camera. The excitation wavelength was 430 nm. In the case of the PS I-core preparation, a slow fluorescence decay component is observed in the 670−680 nm wavelength region. This slowly decaying fluorescence component contributes to the band in the shorter wavelength side of the slowest DAS in Figure 4A,B and is considered mainly due to the uncoupled Chl's. The decay time of this slow fluorescence component showed almost no temperature dependence. On the other hand, the fluorescence decays at around 705 nm became slightly faster upon temperature increases for both samples.

TABLE 1: Kinetic Parameters of the Fluorescence of PS I Samples

condition	component	time constant (ps)	relative area
PS I-core, exc. 430 nm	DAS1	0.2	−0.71 ± 0.05
	DAS2	5.4 ± 0.17	0.56 ± 0.03
	DAS3	22 ± 1.3	0.25 ± 0.02
	DAS4	130 ± 21	0.072 ± 0.013
	DAS5	350 ± 120	0.065 ± 0.097
	DAS6	2300 ± 2100	0.052 ± 0.003
PS I-core, exc. 460 nm	DAS1	0.2	−0.42 ± 0.08
	DAS2	10 ± 0.4	0.62 ± 0.03
	DAS3	50 ± 12	
	DAS4	86 ± 21.1	0.22 ± 0.04
	DAS5	610 ± 630	0.095 ± 0.015
	DAS6	1700 ± 3940	0.057 ± 0.009
FCPI-PS I, exc. 430 nm	DAS1	0.2 fixed	−0.57 ± 0.05
	DAS2	4.7 ± 0.16	0.51 ± 0.03
	DAS3	23 ± 1.0	0.30 ± 0.02
	DAS4	86 ± 5.1	0.13 ± 0.01
	DAS5	480 ± 24	0.060 ± 0.002
FCPI-PS I, exc. 460 nm	DAS1	0.2, fixed	
	DAS2	0.70 ± 0.061	
	DAS3	15 ± 2.1	0.43 ± 0.08
	DAS4	33 ± 3.0	0.13 ± 0.07
	DAS5	110 ± 5	0.29 ± 0.02
	DAS6	680 ± 27	0.16 ± 0.004

Figure 6 shows the temperature dependence of the time-integrated fluorescence spectra of PS I-core excited at 430 nm (A) and 460 nm (B) and that of FCPI-PS I excited at 430 nm (C) and 460 nm (D). Noticeable spectral changes were observed upon temperature increases up to 77 K. The fluorescence emission in the shorter wavelength region and in the long-wavelength tail increased upon a temperature increase from 17 to 77 K. This is in sharp contrast with the cases of PS I containing red Chl's, which show no appreciable temperature dependence of the fluorescence spectra below 77 K. When Chl *a* was selectively excited with a 430 nm laser, the fluorescence spectra had a shoulder around 665 nm, which was not obvious upon 460 nm excitation. We recognized a general tendency, namely, that the peak position of the time-integrated fluorescence spectrum shifts toward the shorter wavelength side for the PS I-core sample and upon Chl *a*-selective excitation.

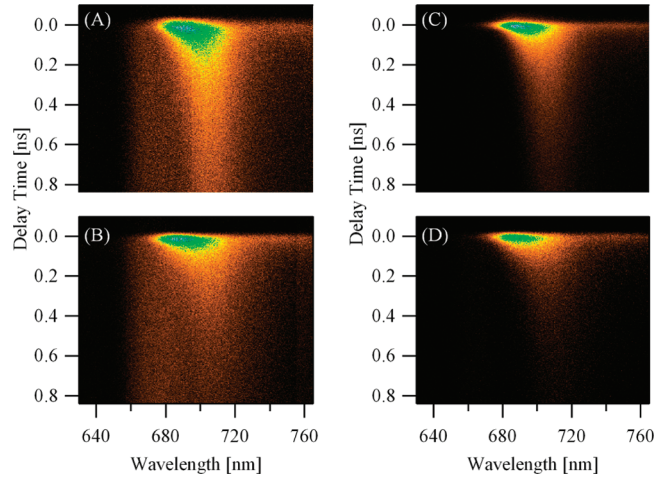

Figure 5. Temperature dependences of the fluorescence 2D images obtained by the streak camera. The signal intensity increases in the order shown by the colors orange, yellow, green, and blue. The left panels show the fluorescence dynamics of the PS I-core preparation excited at 430 nm at 17 K (A) and 77 K (B), and the right panels show those of the FCPI-PS I preparation excited at 430 nm at 17 K (C) and 77 K (D).

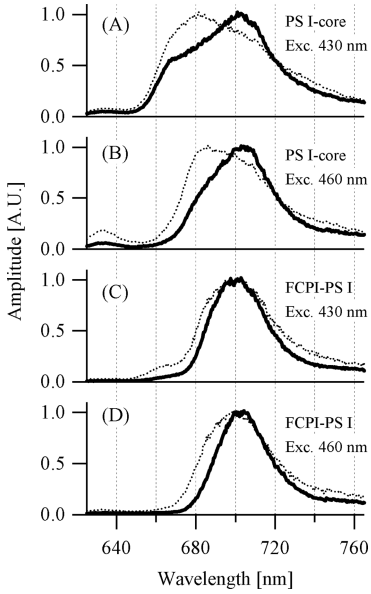

Figure 6. Temperature dependences of the time-integrated fluorescence spectra of PS I-core excited at 430 nm (A) and 460 nm (B) and those of FCPI-PS I excited at 430 nm (C) and 460 nm (D). The thick solid lines and dotted lines are the spectra at 17 and 77 K, respectively.

Discussion

Uncoupled Antenna States in the Diatom PS I-core Complex. Slow fluorescence decays with time constants of ca. 2 ns were detected only in the PS I-core sample upon both 430 and 460 nm excitation. This decay phase is considered to originate from the excited states of pigments that are uncoupled from the excitation energy quenching state, i.e., $P700^+$. Such free Chl's might be located either at the interfacial region between the PS I-core complex and FCPI or within FCPI connected weakly to the core complex. Treatment with a high-concentration detergent in the preparation of the PS I-core sample might suppress the tight connection of some FCPI or Chl's to the core complex. In the previous paper,[17] we assumed the existence of a slow fluorescence decay component in the fluorescence dynamics of the FCPI-PS I preparation at 77 K, although its contribution was very minor. In the present study, on the other hand, we obtained satisfactory results for the fitting of the fluorescence dynamics of the FCPI-PS I preparation without assuming the slow decay component. Thus, the application of anion-exchange chromatography instead of gel filtration resulted in a significantly reduced free-Chl content in FCPI-PS I.

Parts A and B of Figure 4 show that the DAS with ca. 2 ns time constants, depicted by black lines, has two separate peaks at around 680 and 710 nm. The latter peak at around 710 nm might be due to the free Chl's within the core complex, because such a fluorescence band was absent in the isolated FCPI.[6] The peak position of the former band corresponds to that of the emission band of isolated FCPI[6] and depends on the excitation wavelength; it was at around 670 nm upon 430 nm excitation and at around 680 nm upon 460 nm excitation. This suggests that FCPI contains two pigment subgroups; one emits fluorescence at around 670 nm and the other at around 680 nm.

At any rate, the integrated areas of these DAS components are very small. Therefore, the free pigments have only a minor contribution to the overall light-harvesting kinetics. This is validated by the fact that the DAS profiles of PS I-core containing some extent of free Chl's were essentially the same as those of FCPI-PS I containing a negligible free-Chl contribution in the case of the excitation at 430 nm. Thus, we interpret in the following that the free Chl's have only a minor contribution to the overall fluorescence dynamics in the PS I-core complex. Although the free Chl's hardly affect the fluorescence dynamics as suggested above, they significantly contribute to the time-integrated fluorescence spectra shown in Figure 6A,B. Shoulder peaks are observed at around 670 and 680 nm, respectively, in Figure 6A,B. These fluorescence bands come from the different free-Chl pools. The shoulder peaks become more conspicuous at 77 K, reflecting the relative decrease of the fluorescence quantum yield of the active antenna at around 700 nm at higher temperature. The temperature dependence of the fluorescence dynamics of the active antenna will be discussed in more detail in the following section.

Light-Harvesting Kinetics within the Core Complex of Diatom PS I. We discuss the light-harvesting dynamics within the core complex mainly on the basis of the experimental data obtained by the excitation at 430 nm. The fluorescence dynamics of the diatom PS I samples excited at 430 nm should be partly contributed from the EET process related to the peripheral antenna pigments because of the remaining FCPI in the present preparations. The numbers of Chl *a* molecules contained in FCPI per P700 were estimated to be 110 and 156 for the PS I-core and FCPI-PS I samples, respectively.[6] We use supplementarily the data of the ultrafast fluorescence dynamics of *T. elongatus* PS I studied in a previous study.[24]

In the cases of 430 nm excitation, the fastest DAS components with a time constant of 0.2 ps were negative over the whole spectral range studied and had negative peaks at around 690 nm. This time constant was almost identical to the instrumental response time and was then fixed to 0.2 ps in the present analysis. We interpreted the 0.2 ps DAS in the cases of 430 nm excitation to be mainly due to the internal conversion process from the directly excited Soret to Q_y state.

The main decay component in both PS I-core and FCPI-PS I excited at 430 nm was manifested by the DAS component with the second fastest time constants of ca. 5 ps (shown by red lines), with a peak at around 700 nm. The large relative area of this component shown in Table 1 indicates that it accounts for more than 50% of the overall fluorescence decay process. We revealed in a previous paper that the fluorescence dynamics of PS I of *T. elongatus* at 15 K is also dominated by a DAS component with a decay time of 6.1 ps.[24] Although the 6.1 ps DAS component of *T. elongatus* PS I had a peak position at a much longer wavelength of 740 nm due to the major contribution of the red Chl, its time scale was quite similar to that of the dominant DAS component of *C. gracilis* PS I upon 430 nm excitation. Figure 4 also shows that both the PS I-core and FCPI-PS I samples have DAS components with time constants of ca. 100 ps (ranging from 86 to 130 ps, shown by orange lines) and ca. 400 ps (ranging from 350 to 680 ps, shown by blue lines). Our previous work has shown the existence of DAS components in PS I of *T. elongatus* with time constants similar to those of the two DAS components described above. Although the peak positions of the DAS components of *T. elongatus* PS I were again in the region of the red Chl-emitting wavelength, their decay times were in nice agreement with those of *C. gracilis* PS I.

To illustrate the similarity in the distribution of the decay times between the diatom and cyanobacterial PS I, in Figure 7, we plot the relative area of DAS components vs their time constants. In Figure 7, we compare the decay time distribution of PS I-core excited at 430 nm (closed bars) with that of PS I of *T. elongatus* (open bars). The DAS components with time

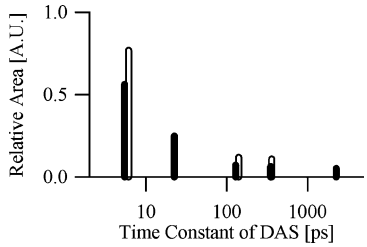

Figure 7. Black closed bars indicate the relative area of the DAS of PS I-core excited at 430 nm plotted vs the time constants. The open bars show that of PS I of *T. elongatus* at 15 K.

constants of 22 ps and 2.3 ns were observed only in *C. gracilis* PS I. On the other hand, the other three DAS components of *C. gracilis* PS I with time constants of 5.4, 130, and 350 ps have corresponding counterparts in *T. elongatus* PS I with similar relative areas and time constants. Our interpretation of the EET pathway in *T. elongatus* PS I is as follows:[24] the photon energy captured by any single antenna state is first funneled into one of the three red Chl's and then transferred to $P700^+$. EET from the three red Chl's to $P700^+$ is responsible for the three DAS components. The difference in the decay times reflects the different distances and mutual orientation of the transition dipole vectors between the red Chl and $P700^+$. The relative area of each DAS component can be a measure of the number of antenna Chl molecules that funnel the excitation energy to the corresponding red Chl.

The similar decay time distributions between *C. gracilis* PS I and *T. elongatus* PS I imply similar EET pathways in PS I of the two organisms. The excitation energy in *C. gracilis* PS I is considered to be first funneled into one of three antenna states, hereafter called a "terminal antenna", which then transfers the energy to $P700^+$. The terminal antennae are red Chl's in *T. elongatus* PS I, while their fluorescence bands are located in the region of 690−710 nm in *C. gracilis* PS I. Similar time constants suggest that Chl molecules forming the terminal antennae are located at similar positions in PS I of the two organisms.

Although the molecular identity of red Chl's in PS I has not yet been established, several candidates have been proposed. A theoretical study by Sener et al. proposed the dimeric Chl's A32−B7, A33−A34, A24−A35, and B22−B34 as the probable candidates.[31] Here, we used the nomenclature of Jordan et al.[32] for Chl naming. Another theoretical study by Damjanović et al. speculated that A32−B7, B24−B25, and A26−A27 were responsible for the red Chl's.[33] On the basis of our experimental results of the ultrafast fluorescence measurement, we proposed that A32−B7 and A33−A34 are possibilities for assignment to the red Chl's.[24] The currently available amino acid sequences of the diatoms are those of *Thalassiosira pseudonana*.[34,35] This diatom is also known to have PS I lacking red Chl's.[6,36] The amino acid residues that serve as ligands to the red Chl candidates described above are well conserved among various organisms, including *Th. pseudonana*. This might not suggest an incorrect assignment of the red Chl's but implies that the red shifts of Chl emission bands are induced by factors other than the ligand-serving amino acid residue.

According to the above interpretation, we present in Figure 8 a schematic description of the EET pathway of the diatom PS I. In the core complex, there are three putative terminal antenna states which have EET rates to $P700^+$ of ca. 5, ca. 100, and ca. 400 ps and have emission peaks at around 700, 700, and 710 nm, respectively. The terminal antennae are depicted by black closed squares in Figure 8. The Chl's in the core

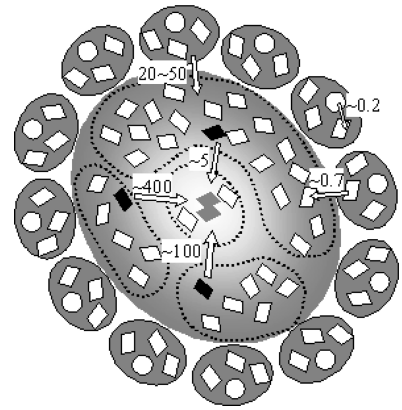

Figure 8. Schematic description of the light-harvesting pathway in *C. gracilis* PS I at 17 K. The large ellipsoid indicates the core complex, and the small ones surrounding the core complex indicate FCPI. Open squares and black closed squares are antenna Chl *a* and terminal antenna, respectively. The two closed gray squares at the center show the special pair, which is in the oxidized form, $P700^+$, in the present study. The open circles in FCPI indicate Chl *c*. The dashed closed curves represent the groups of antenna Chl *a* tightly coupled to each other. The arrows and numbers alongside them indicate the energy flows and their time constants.

complex are divided into four groups, as depicted by the dashed closed curves. The group at the center contains P700 and forms the electron-transfer chain. Each of the other three groups contains one terminal antenna. The excitation energy is first funneled into the terminal antenna in the group and then transferred to $P700^+$.

Light-Harvesting Kinetics of Diatom PS I Related to the Peripheral Antenna. Figure 7 shows a DAS component with a time constant of 22 ps in PS I-core excited at 430 nm, which was absent in *T. elongatus* PS I. We speculate that this 22 ps DAS component corresponds to the EET process from the Chl *a* molecules in FCPI to $P700^+$ through the terminal antenna that transfers the excitation energy to $P700^+$ with a 5 ps time constant. A DAS with essentially the same time constant of 23 ps is also obtained in FCPI-PS I excited at 430 nm. The above interpretation is consistent with the fact that the relative area of this DAS component was larger for FCPI-PS I having a larger amount of FCPI attached. However, we cannot exclude the possibility that the 22 ps DAS component originates from the excitation energy trapping from a terminal antenna within the core complex, which is specific for diatom PS I. To examine this possibility, experiments with a completely FCPI free PS I preparation are necessary.

The 460 nm laser irradiation results in exclusive excitation of both Chl *c* and fucoxanthin contained only in FCPI. Thus, we can deduce the light-harvesting kinetics related to FCPI by examining the difference in the fluorescence dynamics obtained by the 430 and 460 nm excitations. Unfortunately, our excitation condition could not selectively excite either Chl *c* or fucoxanthin. In the present investigation with the 460 nm excitation, thus, we could deduce the energy-transfer dynamics containing the mixed contributions from these two pigments. We recognize 0.2 ps DAS components showing an EET nature from 630 to 680 nm in the data of both PS I-core and FCPI-PS I samples excited at 460 nm. This component is clearly due to EET from Chl *c* to Chl *a* in FCPI. The internal conversion process from the Soret to Q_y state and/or energy transfer through fucoxanthin is probably mixed with this component. EET in the isolated FCP at room temperature has already been reported by Papagiannakis et al.[37] Our result is consistent with their report, which

revealed the time constant of EET from Chl *c* to Chl *a* in FCP to be 100 fs at room temperature.

The FCPI-PS I sample excited at 460 nm has a 0.7 ps DAS component which is negative in the 680−710 nm spectral region. Figure 3, trace d, clearly demonstrates the existence of the 0.7 ps fluorescence rise at 688 nm. In a similar spectral region, the 0.2 ps DAS component of PS I-core excited at 460 nm has a negative peak. Since the isolated FCPI shows a fluorescence emission peak at around 680 nm at 77 K,[6] the 0.7 ps DAS component having a large negative peak at around 700 nm cannot be due to EET within FCPI. We interpret that this 0.7 ps DAS component indicates EET from FCPI to the core complex. This DAS component has only a small positive peak as compared with the large negative band in the 680−710 nm region. We believe that the positive peak of the 0.7 ps DAS component was very small because of the mixing of the negative peak of the 0.2 ps DAS. Since the 0.7 ps component is absent in the PS I-core sample excited at 460 nm, it should reflect the EET from FCPI that is removed in the PS I-core preparation.

The DAS profiles of FCPI-PS I excited at 460 nm with time constants slower than 20 ps are essentially the same as those obtained in the previous study,[17] although the time constants were slightly slower that those at 77 K. The slow >3 ns component reported in the previous study was absent in the present preparation. This indicated that the slightly modified preparation method in the present study resulted in a significant reduction of uncoupled Chl's. Both the PS I-core and FCPI-PS I samples excited at 460 nm showed DASs with time constants of ca. 40 ps (50 ps for PS I-core and 33 ps for FCPI-PS I) showing an EET nature. These DAS components have positive peaks at around 690 nm and negative peaks at around 710 nm, suggesting the EET process from FCPI to the core complex. The corresponding component at 77 K was shown to have a slightly faster time constant of 16 ps.[17] The DAS components with time constants of 110 and 680 ps shown in Figure 4D have spectral profiles similar to those with time constants of 57 and 246 ps in Figure 10 of the previous paper.[17] Thus, these time constants become somewhat slower upon a temperature decrease from 77 to 17 K. Combining all the DAS components discussed above, we give a full schematic description of EET in the PS I complex of the diatom in Figure 8. There are two channels for EET from FCPI to the core complex: one induces the 0.7 ps DAS, and the other induces the ca. 40 ps DAS component.

Shallow-Sink State in the Core Complex of Diatom PS I. The fluorescence spectrum of *C. gracilis* PS I showed a considerable dependence on the temperature even below 100 K as shown in Figure 6. The temperature dependences of the profiles of the time-integrated fluorescence spectra are due to the temperature dependence of the lifetime of the fluorescence at around 705 nm as shown in Figure 5. The fluorescence band at around 705 nm is emitted from the terminal antenna state. Since the fluorescence band of the terminal antenna has a relatively slow lifetime ranging from 350 to 680 ps at 17 K, it has a significant contribution to the time-integrated fluorescence spectra. The blue shifts of the time-integrated spectra upon temperature increases shown in Figure 6 are due to the shortening of the lifetime of the terminal antenna fluorescence at around 705 nm.

The terminal antenna with the slowest EET rate to $P700^+$ has an emission peak at a slightly longer wavelength than the bulk Chl's that have the fluorescence peak at around 690 nm. Thus, they should act as a shallow sink in the antenna system within which the excitation energy is trapped only at cryogenic temperature. The excitation energy trapped by the shallow sink escapes from it when the thermal energy overcomes the energy gap between the shallow-sink state and the bulk Chl's. Thus, the fluorescence from the shallow sink decays faster at 77 K. As described in the previous section, the PS I-core sample contains both EET-active and EET-inactive pigment pools. The fluorescence decays of the EET-active pools become faster with a temperature increase because the excitation energy can escape from the shallow sink. The fluorescence quantum yields of the EET-inactive pools are not affected by the temperature increase, and their relative contributions to the time-integrated fluorescence spectra become larger with the temperature increase.

To estimate the peak position of the fluorescence spectrum of the shallow-sink state, we fitted the spectral profiles of DASs of the shallow sink depicted by the blue lines in Figure 4 to single Gaussian bands. The DASs of the shallow sink shown in Figure 4 could be well approximated by single Gaussian bands with peak wavelengths ranging from 705 to 710 nm and values of full widths at half-maximum (fwhm) ranging from 23 to 27 nm (data not shown). The result above suggests the very proximity of the excitation energy of the shallow sink to that of P700. If we assume the position of the excited states of the shallow sink and P700 to be 702 and 696 nm, respectively, the energy difference is estimated to be ca. 140 cm^{-1}. The absorption spectra of the diatom PS I samples at 77 K showed only a small amplitude at around 702 nm, suggesting that a small number of Chl molecules constitute the shallow sink. The very rapid increases of the fluorescence at around 710 nm shown in Figures 2 and 4 indicate that the excited state of the shallow-sink state is populated within the very early phase of light harvesting. This situation is quite similar to that of *T. elongatus* PS I and suggests an extremely efficient energy funneling from many antenna pigments into the shallow sink.

The conspicuous temperature dependence of the fluorescence spectra of the diatom PS I samples is similar to that observed in the light-harvesting process of photosystem II.[38] In the case of PS II, several specific Chl's in CP47 were assigned to have considerably low excitation energies.[39] These Chl's might act as shallow sinks in PS II. On the other hand, the energy difference of the excited states between the red Chl and P700 of *T. elongatus* PS I is roughly estimated to be ca. 400 cm^{-1}. Thus, the excitation energy trapped within the red Chl's cannot escape below 100 K. Thus, the red Chl's act as fairly deep sinks in this case, and then only a very limited temperature dependence of the fluorescence spectrum is observed below 100 K.

Conclusions

The present study revealed a similarity in the light-harvesting kinetics of diatom and cyanobacterial PS I in spite of their considerable difference in the fluorescence peak wavelengths. Here, we emphasize that the experiments at cryogenic temperature in the present study succeeded in revealing the common feature in the light-harvesting pathways of PS I of these two organisms. The present work also revealed two EET phases from FCPI to the core complex with time constants of 0.7 and ca. 40 ps. EET from FCPI to the core complex is quite effective; thus, the selective excitation of Chl *c* in FCPI does not induce a severe retardation of light harvesting in diatom PS I. The rate-limiting step at cryogenic temperature is not EET from FCPI to the core complex but the escape from the shallow-sink antenna state.

The large energy gap of ca. 400 cm^{-1} between the red Chl's and P700 estimated for cyanobacterial PS I results in a rather concentrated excitation energy population on the red Chl's even at room temperature. On the other hand, the shallow-sink state of diatom PS I might have only a minor effect on the overall

excitation dynamics at room temperature. It is an important future issue to elucidate how the unique characteristic of the terminal antenna states of diatom PS I contributes to their specific acclimation mechanisms against the environmental light condition.

Acknowledgment. This work was supported in part by a Grant-in-Aid for Scientific Research (17750010), the 21st COE program for The Origin of the Universe and Matter from the Japanese Ministry of Education, Science, Sports, and Culture (MEXT), and the Japan Society for the Promotion of Science (JSPS).

Supporting Information Available: Figure showing the time profiles of the up-conversion setup obtained by the first, second, third, and fourth scans. This material is available free of charge via the Internet at http://pubs.acs.org.

References and Notes

(1) Field, C. B.; Behrenfeld, M. J.; Randerson, J. T.; Falkowski, P. *Science* **1998**, *281*, 237–240.

(2) Falkowski, P. G.; Katz, M. E.; Knoll, A. H.; Quigg, A.; Raven, J. A.; Schofield, O.; Taylor, F. J. R. *Science* **2004**, *305*, 354–360.

(3) Falkowski, P.; Scholes, R. J.; Boyle, E.; Canadell, J.; Canfield, D.; Elser, J.; Gruber, N.; Hibbard, K.; Högberg, P.; Linder, S.; Mackenzie, F. T.; Moore, B.; Pedersen, T.; Rosenthal, Y.; Seitzinger, S.; Smetacek, V.; Steffen, W. *Science* **2000**, *290*, 291–296.

(4) Guglielmi, G.; Lavaud, J.; Rousseau, B.; Etienne, A. L.; Houmard, J.; Ruban, A. V. *FEBS J.* **2005**, *272*, 4339–4348.

(5) Durnford, D.; Aebersold, R.; Green, B. *Mol. Gen. Genet.* **1996**, *253*, 377–386.

(6) Ikeda, Y.; Yamagishi, A.; Komura, M.; Kashino, Y.; Shibata, Y.; Itoh, S.; Koike, H.; Satoh, K. Manuscript in preparation.

(7) Falkowski, P. G.; Owens, T. G.; Ley, A. C.; Mauzerall, D. C. *Plant Physiol.* **1981**, *68*, 969–973.

(8) Smith, B. M.; Melis, A. *Plant Cell Physiol.* **1988**, *29*, 761–769.

(9) Demmig-Adams, B. *Biochim. Biophys. Acta* **1990**, *1020*, 1–24.

(10) Olaizola, M.; Yamamoto, H. Y. *J. Phycol.* **1994**, *30*, 606–612.

(11) Arsalane, W.; Rousseau, B.; Duval, J. C. *Photochem. Photobiol.* **1994**, *60*, 237–243.

(12) Kashino, Y. *J. Chromatogr., B* **2003**, *797*, 191–216.

(13) Pyszniak, A. M.; Gibbs, S. P. *Protoplasma* **1992**, *166*, 208–217.

(14) Falciatore, A.; Bowler, C. *Annu. Rev. Plant Biol.* **2002**, *53*, 109–130.

(15) Wilhelma, C.; Büchel, C.; Fisahn, J.; Goss, R.; Jakob, T.; LaRoche, J.; Lavaud, J.; Lohr, M.; Riebesell, U.; Stehfest, K.; Valentin, K.; Kroth, P. G. *Protist* **2006**, *157*, 91–124.

(16) Martinson, T. A.; Ikeuchi, M.; Plumley, F. G. *Biochim. Biophys. Acta* **1998**, *1409*, 72–86.

(17) Ikeda, Y.; Komura, M.; Watanabe, M.; Minami, C.; Koike, H.; Itoh, S.; Kashino, Y.; Satoh, K. *Biochim. Biophys. Acta* **2008**, *1777*, 351–361.

(18) Holzwarth, A. R.; Schatz, G.; Brock, H.; Bittersmann, E. *Biophys. J.* **1993**, *64*, 1813–1826.

(19) Melkozernov, A. N.; Lin, S.; Blankenship, R. E. *Biochemistry* **2000**, *39*, 1489–1498.

(20) Croce, R.; Dorra, D.; Holzwarth, A. R.; Jennings, R. C. *Biochemistry* **2000**, *39*, 6341–6348.

(21) Gobets, B.; van Stokkum, I. H. M.; van Mourik, F.; Dekker, J. P.; van Grondelle, R. *Biophys. J.* **2003**, *85*, 3883–3898.

(22) Koenig, F.; Schmidt, M. *Physiol. Plant.* **1995**, *94*, 621–628.

(23) Lin, S.; Knox, R. S. *Photosynth. Res.* **1991**, *27*, 157–168.

(24) Shibata, Y.; Yamagishi, A.; Kawamoto, S.; Noji, T.; Itoh, S. *J. Phys. Chem. B* **2010**, *114*, 2954–2963.

(25) Shibata, Y.; Kawamoto, S.; Satoh, Y.; Itoh, S. *Photosynth. Res.* **2007**, *91*, 143–143.

(26) Shibata, Y.; Murai, Y.; Satoh, Y.; Fukushima, Y.; Kajima, K.; Ikeuchi, M.; Itoh, S. *J. Phys. Chem. B* **2009**, *113*, 8192–8198.

(27) Sétif, P.; Bottin, H. *Biochemistry* **1989**, *28*, 2689–2697.

(28) Byrdin, M.; Rimke, I.; Schlodder, E.; Stehlik, D.; Roelofs, T. A. *Biophys. J.* **2000**, *79*, 992–1007.

(29) Ke, B. *Arch. Biochem. Biophys.* **1972**, *152*, 70–77.

(30) Pålsson, L. O.; Flemming, C.; Gobets, B.; van Grondelle, R.; Dekker, J. P.; Schlodder, E. *Biophys. J.* **1998**, *74*, 2611–2622.

(31) Sener, M. K.; Lu, D. Y.; Ritz, T.; Park, S.; Fromme, P.; Schulten, K. *J. Phys. Chem. B* **2002**, *106*, 7948–7960.

(32) Jordan, P.; Fromme, P.; Witt, H. T.; Klukas, O.; Saenger, W.; Krauss, N. *Nature* **2001**, *411*, 909–917.

(33) Damjanović, A.; Vaswani, H. M.; Fromme, P.; Fleming, G. R. *J. Phys. Chem. B* **2002**, *106*, 10251–10262.

(34) Armbrust, E. V.; Berges, J. A.; Bowler, C.; Green, B. R.; Martinez, D.; Putnam, N. H.; Zhou, S. G.; Allen, A. E.; Apt, K. E.; Bechner, M.; Brzezinski, M. A.; Chaal, B. K.; Chiovitti, A.; Davis, A. K.; Demarest, M. S.; Detter, J. C.; Glavina, T.; Goodstein, D.; Hadi, M. Z.; Hellsten, U.; Hildebrand, M.; Jenkins, B. D.; Jurka, J.; Kapitonov, V. V.; Kröger, N.; Lau, W. W. Y.; Lane, T. W.; Larimer, F. W.; Lippmeier, J. C.; Lucas, S.; Medina, M.; Montsant, A.; Obornik, M.; Parker, M. S.; Palenik, B.; Pazour, G. J.; Richardson, P. M.; Rynearson, T. A.; Saito, M. A.; Schwartz, D. C.; Thamatrakoln, K.; Valentin, K.; Vardi, A.; Wilkerson, F. P.; Rokhsar, D. S. *Science* **2004**, *306*, 79–86.

(35) Oudot-Le Secq, M. P.; Grimwood, J.; Shapiro, H.; Armbrust, E. V.; Bowler, C.; Green, B. R. *Mol. Genet. Genomics* **2007**, *277*, 427–439.

(36) Ikeda, Y.; Kashino, Y.; Koike, H.; Satoh, K. Purification and the antenna size of photosystem I complexes from a centric diatom, *Chaetoceros gracilis*. In *Photosynthesis. Energy from the Sun*; Allen, J. F., et al., Eds.; Springer: Dordrecht, The Netherlands, 2008; pp 269−272.

(37) Papagiannakis, E.; van Stokkum, I. H. M.; Fey, H.; Büchel, C.; van Grondelle, R. *Photosynth. Res.* **2005**, *86*, 241–250.

(38) Komura, M.; Shibata, Y.; Itoh, S. *Biochim. Biophys. Acta* **2007**, *1757*, 1657–1668.

(39) Raszewski, G.; Renger, T. *J. Am. Chem. Soc.* **2008**, *130*, 4431–4446.

JP102205V